Cost and Benefit Optimization on Installation of Distribution Feeders Voltage Control Equipment considering Distributed Generations

Nien-Che, Yang*, National Taiwan University of Science and Technology, Taiwan
Kuan-Yu Liu, Industrial Technology Research Institute, Taiwan
Wei-Chih Tseng, Yuan Ze University, Taiwan
Hsing-Chih Chen, Industrial Technology Research Institute, Taiwan
Ting-Yen Hsieh, Industrial Technology Research Institute, Taiwan

The Asian Conference on Sustainability, Energy and the Environment 2019
Official Conference Proceedings

Abstract
The primary purpose of this study is to explore the impacts of distributed generation (DG) interconnections on distribution systems in Taiwan. To build a DG-friendly distribution system for the development of DGs, a genetic algorithm with Pareto optimality is utilized to analyze the cost and benefit of installing a distribution feeder voltage control equipment that considers DGs. The major objectives include minimizing the total cost of installing the distribution feeder voltage control equipment and maximizing DG utilization. The total cost includes the installation cost and operation cost of the voltage control equipment. The results indicate that the voltage control equipment is important for improving the voltage profile along the feeders, reducing the system power losses, and maximizing the possible installed capacity of DGs. The conclusions from this study are crucial to DG interconnections and for promoting the future development of renewable energy in Taiwan.

Keywords: Distributed Generation, Voltage Control, Genetic Algorithm.

I. Introduction

According to the governmental policy in Taiwan, hybrid power generation of renewable energy will increase from the present 4.6% to 20% by 2025. When the amount of renewable energy power generation increases significantly, the power quality and the stability of power grid operations are affected. To explore the impacts of distributed generation (DG) interconnections on distribution systems in Taiwan, the voltage deviations of all system buses in the distribution systems are evaluated. The standard of voltage deviation is 0.95–1.03 p.u., according to the Taipower interconnection grid codes. The benefits of installing distribution feeder voltage control equipment and the techniques of reactive power device control (RPDC) used in Taipower were evaluated.

In previous studies [1-4], the voltage deviations of all buses could not satisfy the requirements of grid codes under some scenarios. That is, the voltage control equipment installed at the substation could regulate the voltages at the secondary side of the substation transformer. Because of this drawback of RPDC, an automatic voltage regulator (AVR) is an economical solution to improve voltage deviations along feeders. In this study, an automatic voltage regulator is utilized to improve the voltage profile along feeders. System index factors such as voltage deviations, operation sequences of RPDC, and maximum permissible capacity of DGs are calculated after performing power flow solutions.

II. Proposed Algorithm

The maximum permissible capacity of DGs is restricted by the limitations of steady-state voltage deviations caused by the DG interconnection and maximum continuous operating current of the feeder [5-9]. To reduce this steady-state voltage deviation, utilizing a feeder voltage control equipment is a reasonable solution to maintain the node voltages along a distribution feeder within a permissible range. Hence, the impact assessment for DG interconnections, and cost and benefit optimizations for the sizing and siting of voltage control equipment are proposed in this paper.

2.1 Impact assessment for DG interconnection

To evaluate the impact of DGs on distribution systems, the Monte-Carlo-based power flow method is used in this study. In the feasible regions of interest of the distribution systems, the possible combinations of system topologies and load states, such as (1) system short-circuit capacity, (2) rated capacity of the main transformer, (3) percent impedance of the main transformer, (4) size of the feeder primary conductor, (5) length of the primary feeder, (6) discrete loads along the feeder, (7) power factors of feeder loads, and (8) distribution of feeder loads, are generated. The flowchart of the impact assessment for the DG interconnections is shown in Fig. 1. The calculation procedure is described as follows: (1) set voltage level, (2) set steady-state voltage deviation limitations, (3) set initial system topologies, (4) set feasible region of system parameter data, (5) set number of simulations, (6) initialize system parameters randomly, (7) search the maximum permissible DG capacity by the maximum allowable DG capacity calculation algorithm (MADCCA), (8) regulate feeder voltages by RPDC, and (9) output the results.

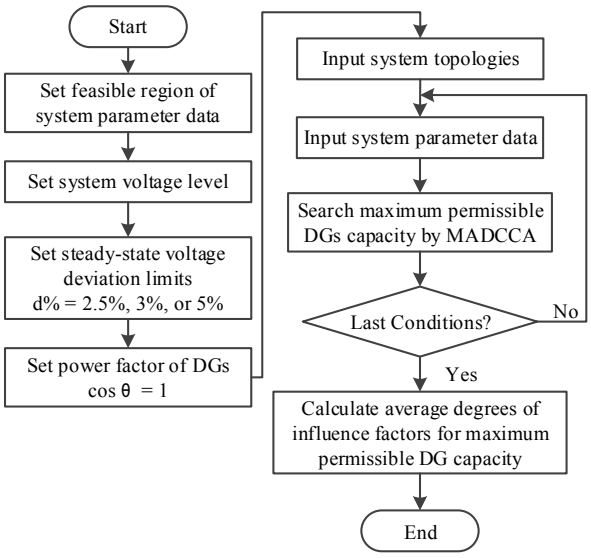

Figure 1: Flowchart of impact assessment for DG interconnection.

The MADCCA is necessary for the calculation procedure described as follows: (1) initial estimate of the maximum permissible DG capacity, (2) power flow calculation, (3) estimation of voltage deviation, and (4) modification of the maximum permissible DG capacity for the next trail value. The flowchart for the MADCCA is shown in Fig. 2.

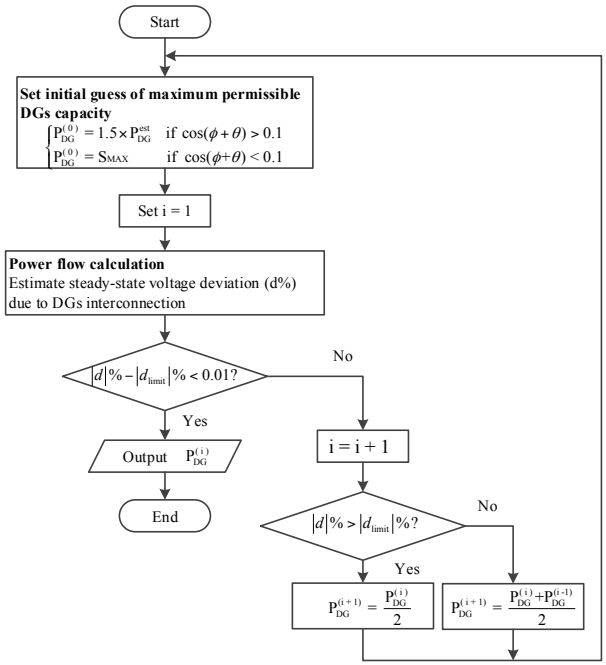

Figure 2: Flowchart for maximum permissible DG capacity calculation algorithm.

2.2 Genetic Algorithm

To optimize the sizing and siting of the voltage control equipment, a genetic algorithm (GA)-based method with a Pareto front is developed. For the proposed method, the sizing and siting of AVRs are the control variables. The first objective is to establish a cost function for searching the minimum cost after installing the AVRs. The second objective is to establish a benefit function for searching the maximum increase in the maximum permissible DG capacity after installing the AVRs. The

flowchart of the proposed GA-based method with a Pareto front is shown in Fig. 3. The solution procedure is described as follows: (1) input the feasible region of system parameters and iteration constraints, (2) initialize the coefficients for the proposed algorithm, (3) set the probabilities of crossover and mutation, (4) estimate the fitness for every individual within the populations, (5) perform elitism, crossover, and mutation between individuals, and reproduce the next-generation populations (6) re-estimate the fitness for every individual within the populations, and (7) verify the stopping rules.

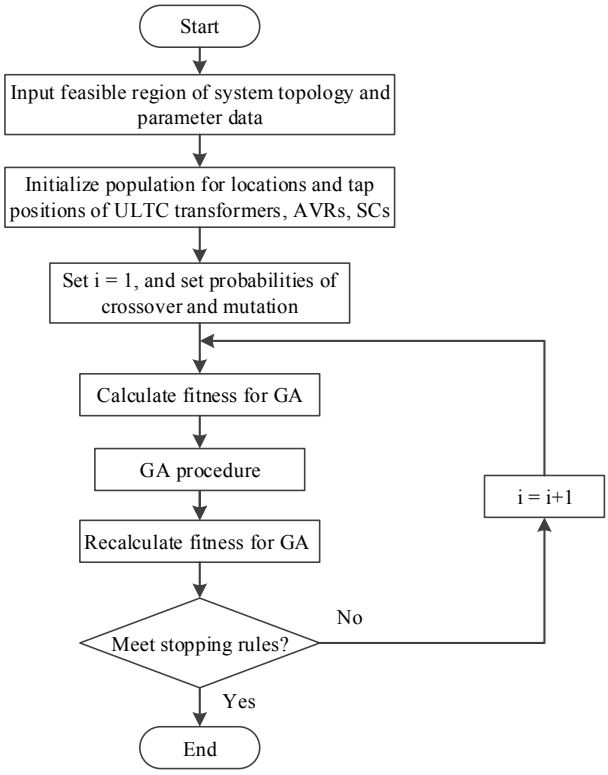

Figure 3: Flowchart of GA-based method with Pareto front for sizing and siting of voltage control equipment.

2.3 Pareto Optimality

Generally, optimization problems can be divided into single- and multiobjective problems. In single-objective optimization problems, an objective function is used for searching a single optimization solution. In multiobjective optimization problems, various objective functions are minimized simultaneously; however, some objectives may conflict with one another, and no single solution can minimize all objectives simultaneously. Hence, a set of nondominated solutions, called Pareto optimal solutions, is used to find good solutions to multiobjective problems as shown in Fig. 4. Pareto optimality can be described mathematically as follows:

$$\forall i \in \{1,2,\ldots,n_f\}, \quad f_i(\vec{x}_1) \le f_i(\vec{x}_2) \qquad (1)$$

$$\exists j \in \{1,2,\ldots,n_f\}, \quad f_j(\vec{x}_1) < f_j(\vec{x}_2) \qquad (2)$$

If both the abovementioned conditions are satisfied, the solution $\vec{x}_1$ dominates solution $\vec{x}_2$.

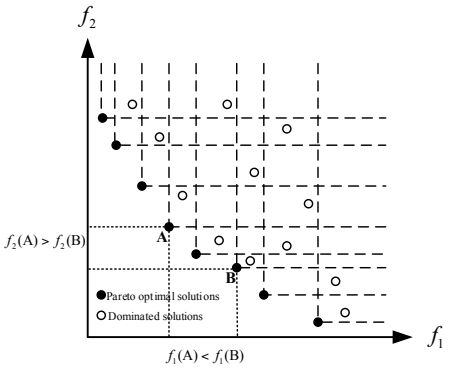

Figure 4: Pareto front for a two-objective problem.

To simulate the impact of DG interconnection on distribution systems, a sample system is used, as shown schematically in Fig. 5. The parameters for the AVR, on-load tap charger (OLTC) transformer, and shunt capacitor (SC) are shown in Tables 1 and 2. The feasible ranges of system parameters for 11.4- and 22.8-kV distribution systems are shown in Tables 3 and 4, respectively. To consider the time-to-time, day-to-day, and season-to-season changes in the load demands and power generations, eight daily characteristic curves are used to represent the power consumption and power generation behaviors for each type of load demand, photovoltaic (PV) generation, and wind generation.

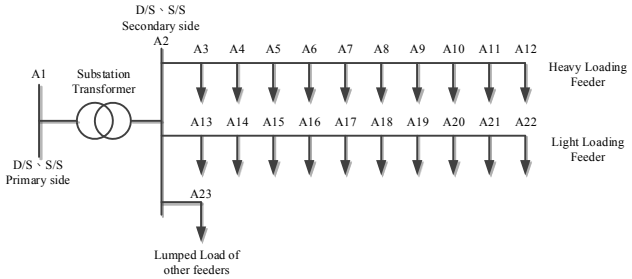

Figure 5: Schematic diagram of the sample system.

Table 1: Parameters for AVR.

Equipment	Parameters
AVR	1. Number of taps: 32 (±16); 2. Controllable voltage for each tap: 0.00625 p.u.; 3. Range of controllable voltage: ±10%

Table 2: Parameters for OLTC transformer and SC.

Equipment	Parameters
OLTC	1. Number of taps: 32 (±16); 2. Controllable voltage for each tap: 0.00625 p.u.; 3. Range of controllable voltage: ±10%
SC	1. Number of capacitor banks: 2 2. Rated capacity of each capacitor bank: 3 Mvar 3. Total rated capacity of capacitor banks: 6 Mvar

Table 3: Feasible ranges of system parameters for 11.4-kV distribution systems

Factor	Parameters
System short-circuit capacity	800 MVA in 69/11.4 kV DSs 2,000 MVA in 161/11.4 kV DSs
X/R ratio of equivalent system impedance	6.0–6.5
Rated capacity of substation transformer	12.5 MVA or 25 MVA in 69/11.4 kV DSs 30 MVA or 60 MVA in 161/11.4 kV DSs
Percent impedance of substation transformer	5–15%
X/R ratio of substation transformer	10–20
Size of primary feeder	477AAC: 0.131 + j0.364 Ω/km
Length of primary feeder	5–12 km
Total loads of a given feeder	600 kW–3 MW
Total loads of other feeders	2–9 MW
Power factor of feeder loads	0.8 lagging–1.0

Table 4: Feasible ranges of system parameters for 22.8-kV distribution systems

Factor	Parameters
System short-circuit capacity	2,000–8,000 MVA
X/R ratio of equivalent system impedance	6.0–6.5
Rated capacity of substation transformer	30 MVA or 60 MVA
Percent impedance of substation transformer	5–15%
X/R ratio of substation transformer	10–20
Size of primary feeder	500 MCM: 0.1469 + j0.1325 Ω/km
Length of primary feeder	5–20 km
Total loads of a given feeder	1.2–6 MW
Total loads of other feeders	4.8–24 MW
Power factor of feeder loads	0.8 lagging–1

2.4 Objective Functions

To ensure voltage quality along feeders and minimize the investment of installing the AVRs, the cost and benefit functions for installing the AVRs are adopted in this study.

(a) Cost function:

Minimize

$$\begin{aligned} f_1 = & \sum_{p=1}^{12}\sum_{l=1}^{n}\sum_{k=1}^{m}\sum_{j=1}^{24}\alpha_1\sum_{i=1}^{N_{AVR}}J_{AVR,i} \\ & +\sum_{p=1}^{12}\sum_{l=1}^{n}\sum_{k=1}^{m}\sum_{j=1}^{24}\alpha_2 C_{main,tap}\left|Tap_{main,after,j}^{k,l,p}-Tap_{main,before,j}^{k,l,p}\right| \\ & +\sum_{p=1}^{12}\sum_{l=1}^{n}\sum_{k=1}^{m}\sum_{j=1}^{24}\alpha_3 C_{cap}\left|N_{Cap,after,j}^{k,l,p}-N_{Cap,before,j}^{k,l,p}\right| \\ & +\sum_{p=1}^{12}\sum_{l=1}^{n}\sum_{k=1}^{m}\sum_{j=1}^{24}\alpha_4 C_{AVR,tap}\left|Tap_{AVR,after,j}^{k,l,p}-Tap_{AVR,before,j}^{k,l,p}\right| \end{aligned} \quad (3)$$

where $J_{AVR,i}$ is the investment cost of the ith AVR (\$); N_{AVR} is the number of AVR; $C_{main,tap}$ is the operating cost of the OLTC transformer (\$/p.u.); C_{cap} is the operating cost of the shunt capacitor (\$/p.u.); $C_{AVR,tap}$ is the operating cost of the AVR (\$/p.u.); $Tap_{main,before,j}^{k,l,p}$, $N_{Cap,before,j}^{k,l,p}$, and $Tap_{AVR,before,j}^{k,l,p}$ are the tap positions of the OLTC transformer, number of shunt capacitors, and tap position of the AVR at the *j*th hour, *l*th day, *p*th month under the *k*th loading condition before installing AVR, respectively; $Tap_{main,after,j}^{k,l,p}$, $N_{Cap,after,j}^{k,l,p}$, and $Tap_{AVR,after,j}^{k,l,p}$ are the tap position of the OLTC transformer, number of shunt capacitors, and tap position of the AVRs at the *j*th hour, *l*th day, *p*th month under the *k*th loading condition after installing the AVRs, respectively; α_1, α_2, α_3, and α_4 are cost weighting coefficients. Here, α_1=300 (*p.u./\$*), α_2=3 (*p.u./\$*), α_3=5 (*p.u./\$*), and α_4=1 (*p.u./\$*)。

(b) Benefit function:

Minimize

$$f_2 = \sum_{p=1}^{12}\sum_{l=1}^{n}\sum_{k=1}^{m}\sum_{j=1}^{24}\beta\cdot(P_{DG,before,j}^{k,l,p}-P_{DG,after,j}^{k,l,p}) \quad (4)$$

$$P_{DG,j} = \gamma_1 P_{PV,j} + \gamma_2 P_{wind,j} \quad (5)$$

where $P_{DG,after,i}^{k,l,p}$ is the permissible capacity of the DGs (MW) at the *j*th hour, *l*th day, *p*th month under the *k*th loading condition after installing the AVRs; $P_{DG,before,i}^{k,l,p}$ is the permissible capacity of the DGs (MW) at the *j*th hour, *l*th day, *p*th month under the *k*th loading condition before installing the AVRs; β is the benefit coefficient for the DGs. Herein, β = 60(*p.u./MW*). $P_{PV,i}$ is the real power generation (MW) of the PV system at the *j*th hour; $P_{wind,i}$ is the real power generation (MW) of the wind power system at the *j*th hour; γ_1 is the ratio of PV power generation to DG power generation, and γ_2 is the ratio of wind power generation to DG power generation.

III. Simulation Results

The simulation results of the cost and benefit optimization for 69/11.4- and 161/11.4-kV distribution systems with DGs are shown in Tables 5 and 6, respectively. Figs. 6 to 11 show the Pareto front obtained using the proposed method for six

scenarios. In most cases, the optimal locations of DGs are along the light loading feeder. In this case, the wide voltage spread between the light loading feeder and heavy loading feeder can be reduced, and the permissible capacity of the DGs can be increased.

Table 5: Multiobjective optimization for sizing and siting of AVRs in 69/11.4-kV distribution systems with DGs

Scenarios	Objective function	Location of AVRs		f_1	f_2
		Feeder	Distance from the transformer (m)	Cost (p.u.)	Benefit (p.u.)
6 MW of DGs at the end of light loading feeder	Minimum cost	Light loading	7,994–8,221	2625	–494,898
	Maximum benefit	Light loading	7,206–7,233	573.75	–561,503
3 MW of DGs at the end of light loading feeder	Minimum cost	Light loading	2,422–3,452	–1616.25	–79,590
	Maximum benefit	Light loading	144–2,321	–1342.5	–86,221
6 MW of DGs at the middle end of light loading feeder	Minimum cost	Light loading	5,388–5,396	–1205.625	–367,697
	Maximum benefit	Light loading	3,921–4,785	–658.125	–532,454

Table 6: Multiobjective optimization for sizing and siting of AVRs in 161/11.4 kV-distribution systems with DGs

Scenarios	Objective function	Location of AVRs		f_1	f_2
		Feeder	Distance from the transformer (m)	Cost (p.u.)	Benefit (p.u.)
6 MW of DGs at the end of light loading feeder	Minimum cost	Light loading	8,304–8,312	163.125	–492,656
	Maximum benefit	Light loading	26–81	5,501.25	–569,163
3 MW of DGs at the end of light loading feeder	Minimum cost	Light loading	2,694–7,152	–247.5	–69,691
	Maximum benefit	Light loading	300–2,312	26.25	–95,699
6 MW of DGs at the middle end of light loading feeder	Minimum cost	Light loading	5701	300	–378,496
	Maximum benefit	Light loading	2,415–3,519	847.5	–581,507

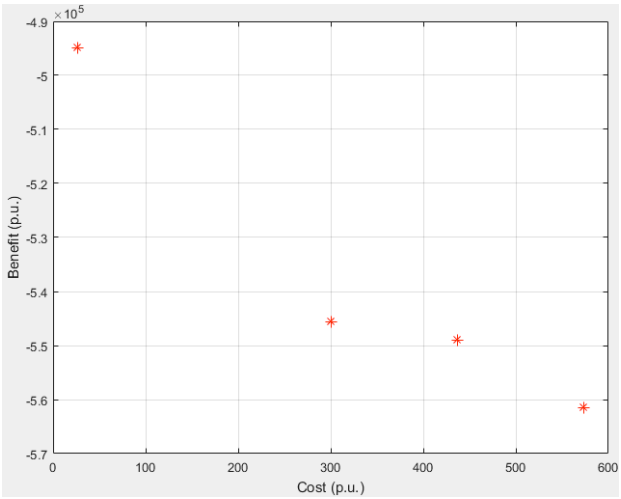

Figure 6: Pareto front for 3 MW of DGs interconnected at the end of light loading feeder (69/11.4-kV distribution systems)

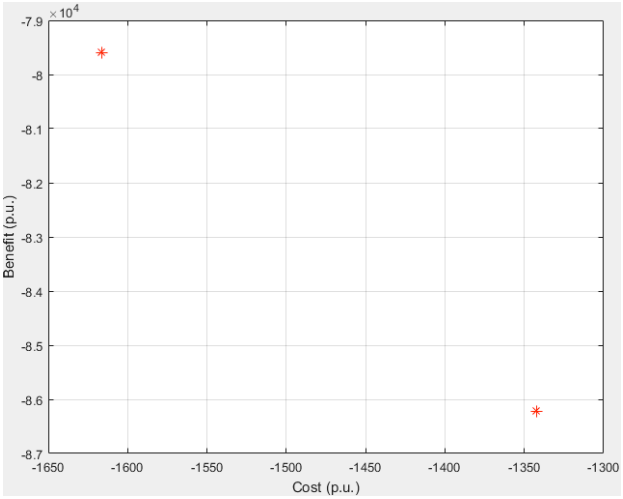

Figure 7: Pareto front for 6 MW of DGs interconnected at the end of light loading feeder (69/11.4-kV distribution systems)

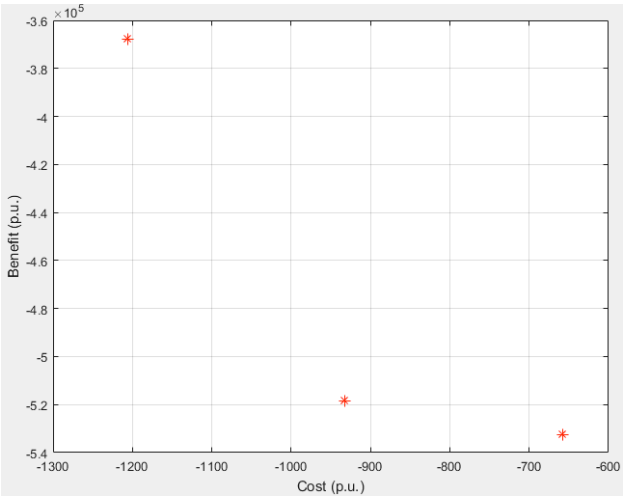

Figure 8: Pareto front for 6 MW of DGs interconnected at the middle of light loading feeder (69/11.4-kV distribution systems)

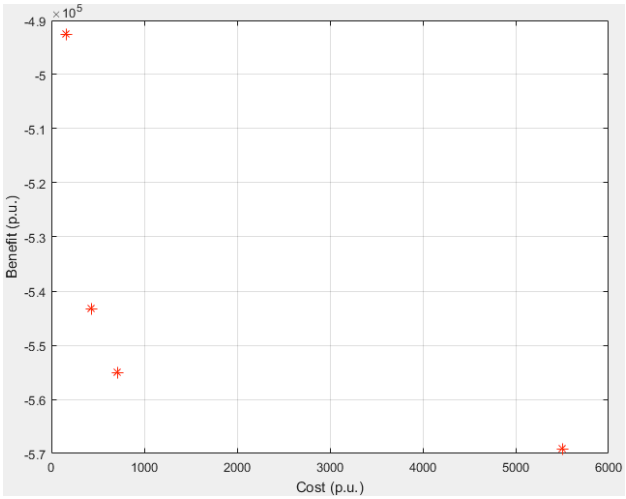

Figure 9: Pareto front for 3 MW of DGs interconnected at the end of light loading feeder (161/11.4-kV distribution systems)

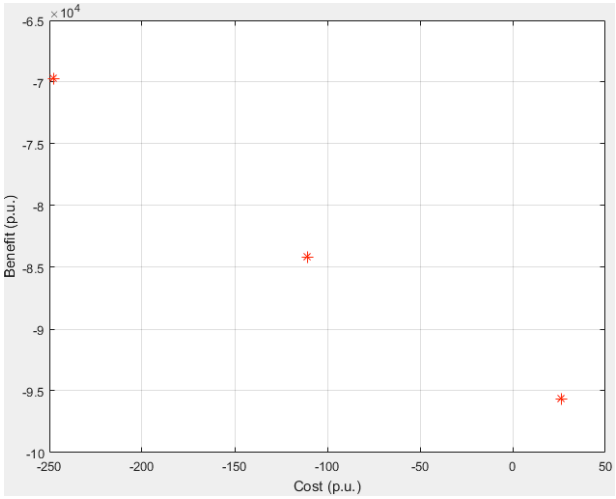

Figure 10: Pareto front for 6 MW of DGs interconnected at the end of light loading feeder (161/11.4-kV distribution systems)

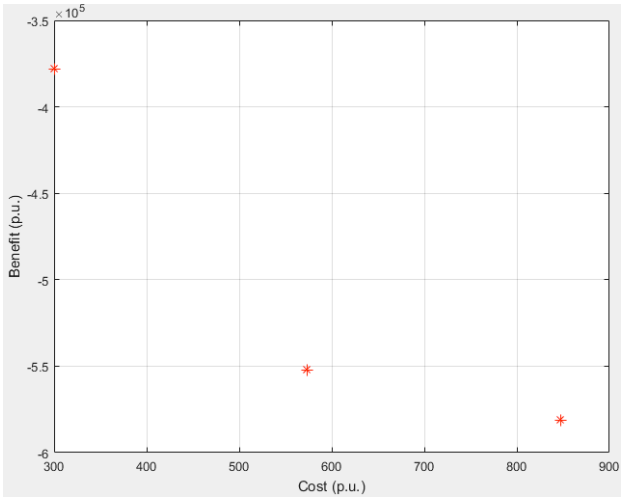

Figure 11: Pareto front for 6 MW of DGs interconnected at the middle of light loading feeder (161/11.4-kV distribution systems)

IV. Conclusion

In this study, the GA based method with Pareto optimality was developed to optimize the cost and benefit of installing an AVR in distribution feeders with DGs. First, the impacts of DG interconnections on distribution systems in Taiwan were investigated. The worst cases were used as sample systems. The primary objectives included minimizing the total cost of installing distribution feeder voltage equipment and maximizing the DGs utilization. The total cost included the installation cost and operation cost of the voltage control equipment. The conclusions from this study are crucial to the DG interconnections and for promoting the future development of renewable energy in Taiwan.

Acknowledgements

This work was financially supported by the Bureau of Energy, Ministry of Economic Affairs under the project of Shalun Green Energy Science City – Project of Verification Platform for Industrial Green Technology. (Project number: 108-D0603)

References

[1] N.-C. Yang and H.-C. Chen. (2018). Decomposed Newton algorithm-based three-phase power-flow for unbalanced radial distribution networks with distributed energy resources and electric vehicle demands. *International Journal of Electrical Power & Energy Systems,* 96, 473-483.

[2] N.-C. Yang and H.-C. Chen. (2017). Three-phase power-flow solutions using decomposed quasi-Newton method for unbalanced radial distribution networks. *IET Generation, Transmission & Distribution,* 11, 3594-3600.

[3] N.-C. Yang. (2016). Three-phase power flow calculations using direct Z BUS method for large-scale unbalanced distribution networks. *IET Generation, Transmission & Distribution,* 10, 1048-1055.

[4] T.-H. Chen, L.-S. Chiang, and N.-C. Yang. (2012). Examination of Major Factors Affecting Voltage Variation on Distribution Feeders. *Energy and Buildings,* 55, 494-499.

[5] G. S, G. SP, and G. S. (2010). Optimal sizing and placement of distributed generation in a network system. *International Journal Electrical Power Energy System,* 32, 849-856.

[6] H. H, N. SA, and A. A. (2008). A method for placement of DG units in distribution networks. *IEEE Transactions on Power Delivery,* 23, 1620-1628.

[7] W. CS and N. MH. (2004). Analytical approaches for optimal placement of distributed generation sources in power systems. *IEEE Transactions on Power Systems,* 19, 2068-2076.

[8] N.-C. Yang and T.-H. Chen. (2011). Evaluation of Maximum Allowable Capacity of Distributed Generations Connected to a Distribution Grid by Dual Genetic Algorithm. *Energy and Buildings,* 43, 3044-3052.

[9] N. C. Yang and T. H. Chen. (2011). Dual Genetic Algorithm-Based Approach to Fast Screening Process for Distributed-Generation Interconnections. *IEEE Transactions on Power Delivery,* 26, 850-858.

Contact email: ncyang@mail.ntust.edu.tw